Cong. Anom., **38:** 67–79,1998

Original

Morphology and Morphometry of the Deformed Cervical Vertebrae in a Mutant *Knotty-Tail (knt/knt)* Mouse

Tetsuro MATSUURA[1], Isao NARAMA[1], Kiyokazu OZAKI[1], Hiroo NAKAJIMA[2], Masahiko NISHIMURA[3], Tomohiro IMAGAWA[4], Hiroshi KITAGAWA[4] and Masato UEHARA[4]

[1]Research Institute of Drug Safety, Setsunan University, 45–1 Nagaotoge-cho, Hirakata, Osaka 573–0101, Japan; [2]Department of Radiation Biology, Osaka University Medical School, 2–2 Yamada-oka, Suita, Osaka 565–0871, Japan; [3]Institute for Experimental Animals, Hamamatsu University School for Medicine, Hamamatsu, Shizuoka 431–3124, Japan; and [4]Department of Veterinary Anatomy, Faculty of Agriculture, Tottori University, Tottori 680–0945, Japan

ABSTRACT Mice with short and knotty tails arose as a spontaneous mutant in an ICR strain, and they have been named *knotty-tail* mouse (gene symbol; *knt*). They also have a minor anomaly of the cervical vertebrae, especially in the axis. In this study, the cervical vertebrae of *knotty-tail* (*knt/knt*) mice were investigated by morphological and morphometric examinations during the prenatal and postnatal period. From the observation of double-stained preparations of *knt/knt* mice, morphological changes of cervical vertebrae were confined to the vertebral arch of the axis, which was asymmetrical and hypoplastic. From the morphometric analyses, outside of the axis, minor anomalies (i.e., broadened cervical vertebrae in the transverse direction, shortened and broadened ventral tuberculum of the atlas, thickened ventral lamina of 6th cervical vertebra) were maintained in the cervical vertebrae of *knt/knt* mice. Morphological deformity, reflecting an adult osseous anomaly, had been already formed in the cartilaginous axis prenatally. In the papain-digested preparations of *knt/knt* mice, a bony invagination into the canal was detected in the axis, and the morphometric analyses on axis revealed that the growth of spinous process was apparently disturbed in comparison with that of ICR mice.

Key words: axis, cervical vertebral anomaly, mouse, spina bifida occulta, vertebral arch

Received August 22, 1997

All correspondence should be addressed to T. Matsuura.
松浦哲郎，奈良間功，尾崎清和，摂南大学　薬物安全科学研究所，〒573-0101　大阪府枚方市長尾峠町45-1
中島裕夫，大阪大学医学部　放射線基礎講座，〒565-0871　大阪府吹田市山田丘2-2
西村正彦，浜松医科大学　実験動物施設，〒431-3124　静岡県浜松市半田町3600
今川智敬，北川浩，上原正人，鳥取大学農学部　獣医学科　家畜解剖学教室，〒680-0945　鳥取県鳥取市湖山町南4丁目101

The *knotty-tail* mouse (gene symbol; *knt*), derived from the ICR strain, has a short, kinked tail with a knot and it also has minor anomalies of the cervical vertebrae, especially in the axis. Genetic data have shown that the *knt* is a simple autosomal recessive gene (Matsuura et al., 1997).

In humans, occipitalization of the atlas and anomalies of the odontoid process are well known as representative cervical vertebral anomalies (Gunther, 1980; Smoker, 1994). Occipitalization of the atlas as an isolated entity is asymptomatic, and an abnormal odontoid process assumes cervical immobility and atlantoaxial instability (Gunther, 1980). Recently, computed tomography (CT) makes it possible to analyze three-dimensional malformations, and new axis anomalies have been precisely detected by CT examination. As a rare anomaly of the human axis, CT reveals spina bifida occulta with a pair of osseous fragments originating from the separated laminae (Koyama et al., 1986), and agenesis of the vertebral arch is also found (Bernini and Muras, 1985).

In animals, there have been many studies on deformities of the odontoid process as well (Theiler, 1951; Searle, 1966; Denny et al., 1977). There are few papers on deformities confined to the vertebral arch of the axis. In only one strain of rabbits a narrow axis is reportedly inherited. However, this strain merely shows a short outer transverse distance of the axis, and no other morphological axis anomalies are detected (Crary and Fox, 1983). Furthermore, there are some mutant mice with complicated cervical deformities involving the axis in which the morphological change is extremely pronounced in comparison with that in humans (Theiler, 1988).

The purpose of this study is to describe the morphological and morphometric analyses of the cervical vertebrae in *knt/knt* mice to elucidate the pre- and postnatal development of the anomalous axis.

MATERIALS AND METHODS

Animals

The progenitors of the mice used in this study were obtained from Hamamatsu University School of Medicine, Hamamatsu, Japan. The mice were housed in air-conditioned animal room, fed standard laboratory diet and supplied water *ad libitum* on a 12-h light and 12-h dark cycle.

For skeletal examinations in this study, a total of 152 mice consisting of 56 male and 16 female offspring, and 20 male fetuses of *knt/knt* mice, together with 30 male and 10 female offspring, and 20 male fetuses of ICR mice, were used. An additional 10 pregnant females of *knt/knt* mice and 6 pregnant females of ICR mice were also used to provide fetuses. Females fetuses were not used for morphological observation of double-stained preparations because there was no sex difference on morphology in the preliminary study.

Skeletal examinations

The animals were anesthetized with ether and sacrificed by exsanguination from the abdominal aorta. Offspring were sacrificed at postpartum weeks 1, 3, 5, 7 and 52. Pregnant females were sacrificed in the same manner on days 15 and 18 of gestation, and fetuses were removed immediately after incision of the uterus. The day on which a vaginal plug was detected was designated day 0 of gestation.

For morphological observation of skeletons, 10 *knt/knt* male fetuses each of 15 and 18 days, 10 males aged 1 week, 9 males aged 3 weeks, 12 males aged 5 weeks and, 7 males aged 7 weeks together with 10 ICR male fetuses each of 15 and 18 embryonic days and 5 males each of 1, 3, 5 and 7 weeks were subjected to double-staining of skeletal specimens with Alizarin Red S and Alcian Blue 8GS prepared by Inouye's method (Inouye,

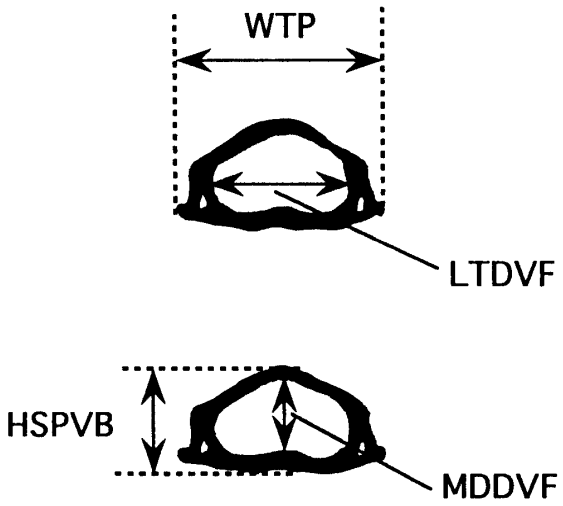

Fig. 1 Measurements of all the cervical vertebrae and their foramen. All cervical vertebrae and their foramen from 52-week-old mice are measured for the width across the transverse processes (**WTP**), the longest transverse diameter of the vertebral foramen (**LTDVF**), the height from the spinous process to the vertebral body (**HSPVB**), and the median dorsoventral diameter of the vertebral foramen (**MDDVF**). Silhouettes show representative measurements of the 3rd cervical vertebra above and below.

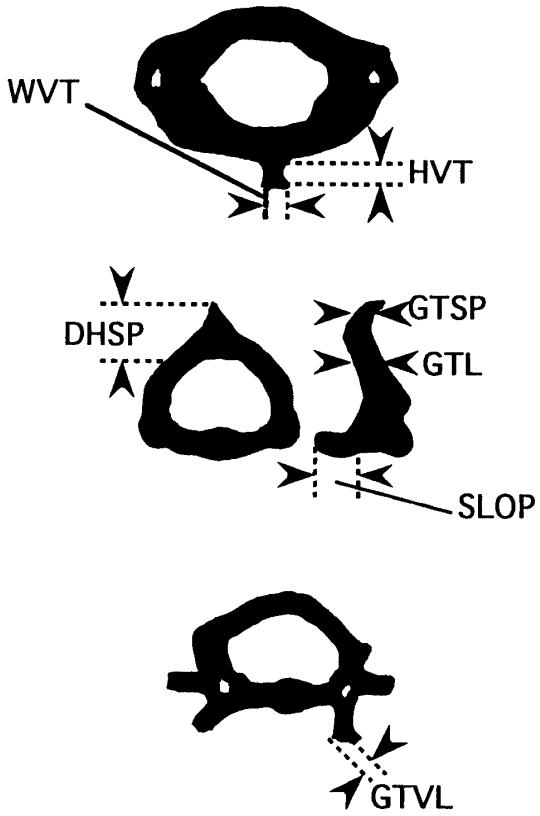

Fig. 2 Measurements of the atlas, the axis and the 6th cervical vertebra. In the atlas from 52-week-old mice, the width (**WVT**) and height (**HVT**) of the ventral tuberculum are measured. In the axis from 5- and 52-week-old mice, the dorsoventral height of the spinous process (**DHSP**) and the greatest thickness of the spinous process (**GTSP**), the greatest thickness of the lamina (**GTL**) and the sagittal length of the odontoid process (**SLOP**) are measured. In the 6th cervical vertebra from 52-week-old mice, the greatest thickness of the ventral lamina (**GTVL**) is measured. Silhouettes show measurements of atlas above, axis in the middle, and 6th cervical vertebra below.

1976).

For morphometric analysis, the axis from another 10 males and 8 females of 5-week-old *knt/knt* mice, and the cervical vertebrae from 8 males and 8 females of 52-week-old *knt/knt* mice, along with 5 males and 5 females each of ICR mice of the same age, were subjected to papain digestion by Luther's method (Luther, 1949). Prior to and after the papain digestion, vertebral specimens or whole skeletons were examined by soft-X-ray film. Confirming the position of each vertebra with soft X-ray film, measurements were made on vertebrae cleaned with papain, using a binocular microscope with a micrometer attachment.

Measurement and quantitative analysis of cervical vertebrae

The details of the measurement method were shown in Fig. 1 and 2. In all the cervical vertebrae and their foramen from 52-week-old mice, overall width and height were measured (Fig. 1). In the atlas from 52-week-old mice, the ventral tuberculum was measured. In the axis from 5- and 52-week-old mice, the spinous process, the lamina and the odontoid process were measured. In the 6th cervical vertebra from 52-week-old mice, the ventral lamina was measured (Fig. 2). Differences were assessed by the analysis of variance and Student's *t* test.

RESULTS

Pre- and postnatal development of the double-stained axis

In 15-day-old *knt/knt* embryos, the cervical vertebrae showed a delay in chondrification. Since the arch of axis had been chondrified in ICR embryos, though not yet in *knt/knt* embryos, it was impossible to discern a morphological anomaly in the cervical vertebrae.

In 18-day-old *knt/knt* embryos, the vertebral arch of the axis has been chondrified but was asymmetrical and hypoplastic, and the paired laminae of the arch often failed to join at the midline. On the other hand, the cartilaginous arch of the axis was symmetrical and homogeneous in ICR embryos (Fig. 3).

At 1–3 weeks, the cartilaginous arches of the cervical vertebrae were gradually ossified in both strains, and the vertebral arch of the axis of *knt/knt* mice was still asymmetrical (Fig. 4).

At 5–7 weeks, the ossification of the axis was largely complete, including the vertebral arches in both strains. The spinous process of axis of *knt/knt* mice was hypoplastic, showing composite grooves on its dorsal surface,

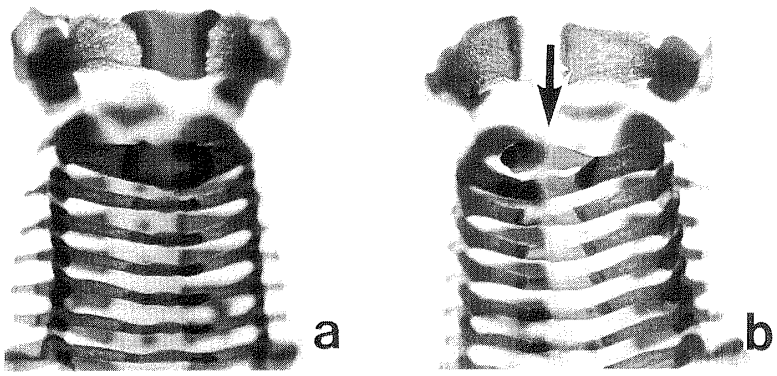

Fig. 3 Cervical vertebrae stained with Alizarin Red S and Alcian Blue in 18-day-old male fetuses. The specimen on the left is normal (a) and the other (b) is that of a *knt/knt* fetus. The vertebral arch of the axis of *knt/knt* fetus is asymmetrical and hypoplastic, with the laminae of the arch failing to join at the midline (*arrow*). ×10.

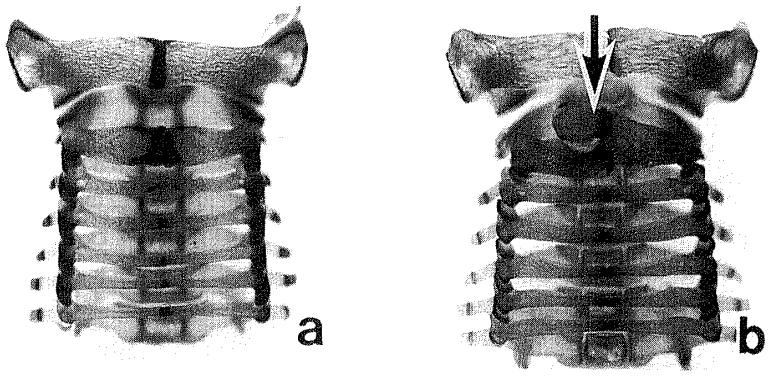

Fig. 4 Cervical vertebrae stained with Alizarin Red S and Alcian Blue in 1-week-old male mice. The specimen on the left (a) is normal and the other (b) is that of a *knt/knt* mouse. The cartilaginous arches of the cervical vertebrae are gradually ossified in both strains, and the vertebral arch of the axis of the *knt/knt* mouse is still asymmetrical (*arrow*). ×6.5.

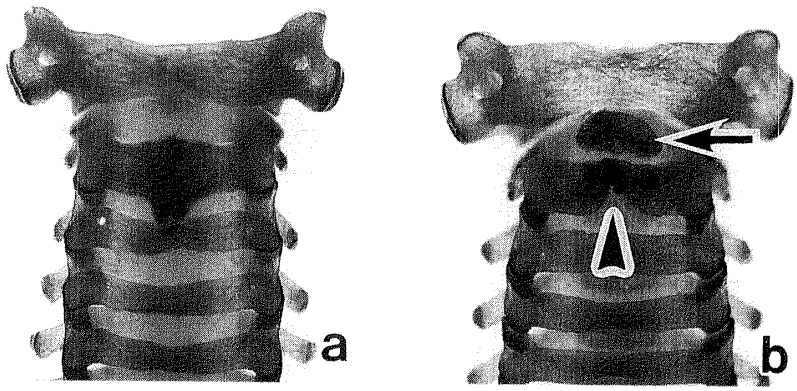

Fig. 5 Cervical vertebrae stained with Alizarin Red S and Alcian Blue in 5-week-old male mice. The specimen on the left (a) is normal and the other (b) is that of a *knt/knt* mouse. The ossification of cervical vertebrae is almost complete, including the vertebral arches in both strains. The spinous process of the axis of *knt/knt* mice is hypoplastic, showing composite grooves on its dorsal surface (*arrowhead*), and the anterior part of the vertebral arch of the axis is completely separated like an island (*arrow*). ×6.5.

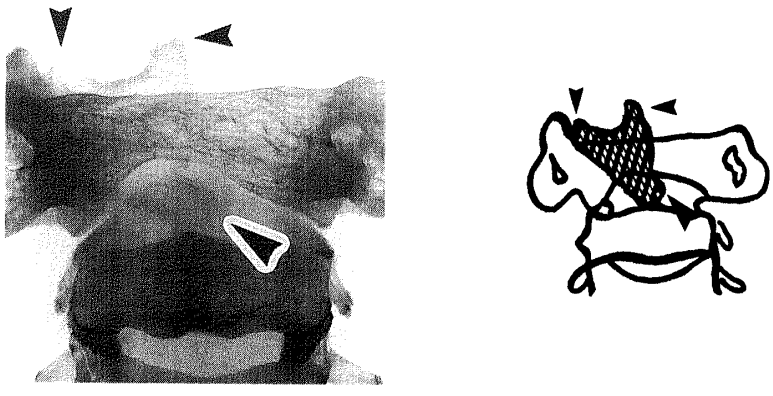

Fig. 6 Cervical vertebrae stained with Alizarin Red S and Alcian Blue in a 7-week-old male *knt/knt* mouse and its diagram. The antero-dorsal part of the vertebral arch protrudes rostrally, and it separates and invades the foramen of the atlas (*arrowhead*, cross-hatched area). ×10.

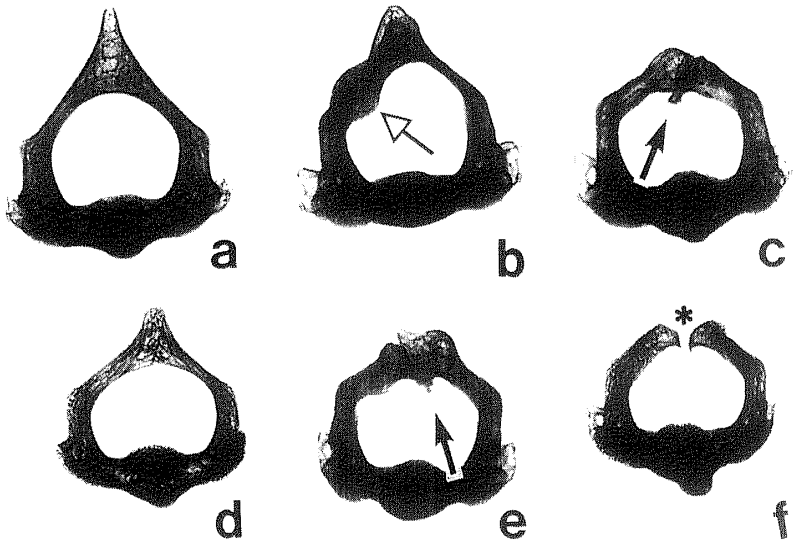

Fig. 7 Structure of the axis indicated by soft X-ray examination in 5- and 52-week-old male mice. The specimens above (a, b, c) are from 52-week-old mice and those below (d, e, f) are from 5-week-old mice. Those on left (a, d) are normal. The others are from *knt/knt* mice in which the hypoplastic and asymmetrical spinous process has some grooves on its dorsal surface. In severe cases, spina bifida occulta (*) is observed. Bony process (*arrow*) or nodular thickening (*open arrow*) invaginate into the vertebral canal from the vertebral arch. ×5.5.

and the anterior part of the vertebral arch of the axis was completely separated like an island (Fig. 5). Furthermore, the antero-dorsal part of the vertebral arch sometimes protruded rostrally, and in severe cases these osseous processes separated from the arch and seemed to compress the spinal cord (Fig. 6).

Morphological and morphometric analyses of papain-digested axis

In papain-digested preparations of 5- and 52-week-old *knt/knt* mice, the axis showed gross deviations. Morphological anomalies of the axis were confined to the vertebral arch, which was usually asymmetrical. The hypoplastic spinous process had some grooves on its dorsal surface. In severe cases, spina bifida occulta was observed. Particularly prominent was the occasional invagination of the bony process into the vertebral canal from the median part of the vertebral arch (Fig. 7).

Morphometric analyses on the axis showed that the dorsoventral height of the spinous process of the axis (DHSP) in both sexes of 5- and 52-week-old *knt/knt* mice was about two-thirds that of normal ICR mice, and the difference was significant at both ages. Moreover, the greatest thickness of the spinous process (GTSP) was significantly narrower in females during the same period. Meanwhile, there was no significant difference in the greatest thickness of the lamina (GTL) or the sagittal length of the odontoid process (SLOP) (Fig. 8).

Morphological and morphometric analyses of other cervical papain-digested preparations

Minor anomalies outside of the axis were detected in the cervical vertebrae of 52-week-old *knt/knt* mice. Morphometric analyses on all the cervical vertebrae and their foramen showed that the width across the transverse process (WTP) and the longest transverse diameter of the vertebral foramen (LTDVF) of *knt/knt* mice were significantly and continuously greater from the 3rd or 4th cervical vertebra to the 7th cervical vertebra

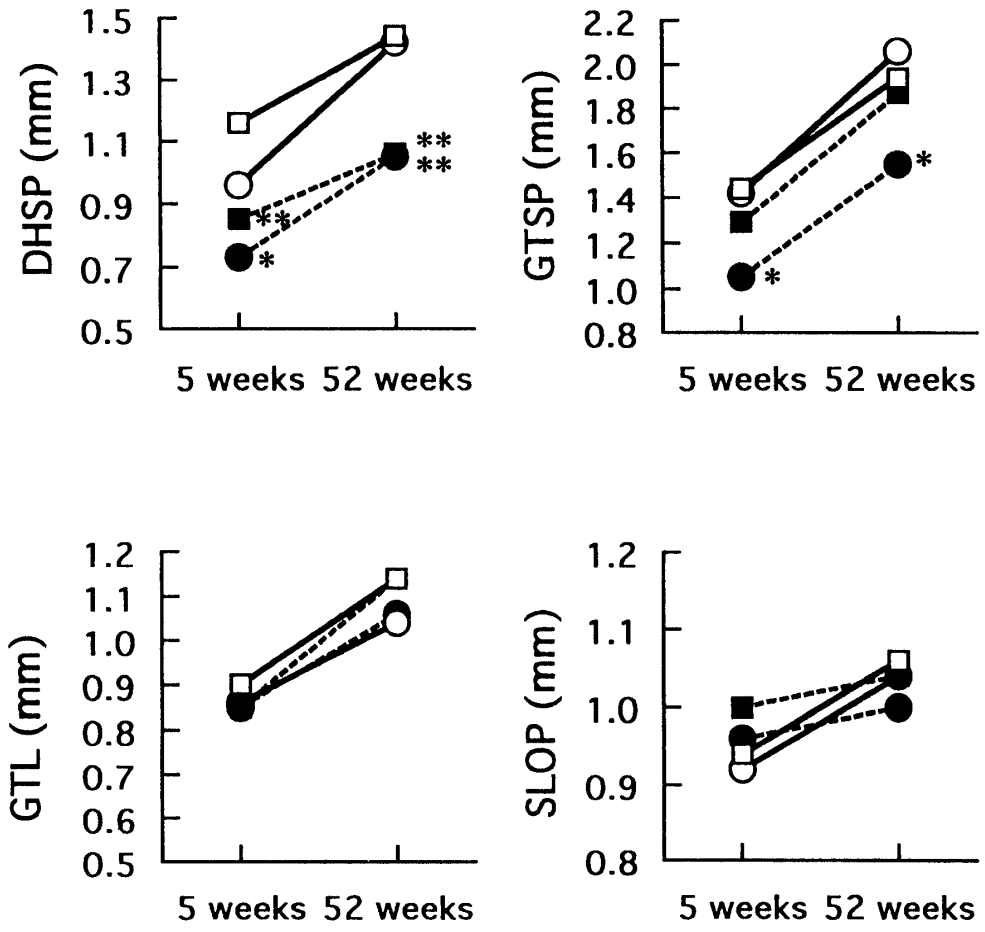

Fig. 8 Morphometric analyses on the axis of 5- and 52-week-old mice.
DHSP, the dorsoventral height of the spinous process; **GTSP**, the greatest thickness of the spinous process; **GTL**, the greatest thickness of the lamina; **SLOP**, the sagittal length of the odontoid process. See Fig. 2. □: male ICR mice; ■: male *knt/knt* mice; ○: female ICR mice; ●: female *knt/knt* mice; *: $P < 0.05$; **: $P < 0.01$ (significant difference from ICR mice). The DHSP in both sexes of 5- and 52-week-old *knt/knt* mice is about two-thirds that of normal ICR mice. The GTSP is significantly narrower in females during the same period. Meanwhile, there is no significant difference in the GTL or the SLOP.

than in ICR mice, and practically common to both sexes. The height from the spinous process to the vertebral body (HSPVB) was also significantly lower in atlas and axis of both sexes, while there was no significant difference in the median dorsoventral diameter of the vertebral foramen (MDDVF) common to both sexes (Fig. 9). Comparing those specimens grossly, the distal halves of cervical vertebrae of *knt/knt* mice seemed to be wider than those of ICR mice (Fig. 10). In the atlas of *knt/knt* mice, the width of the ventral tuberculum (WVT) was nearly twice that of ICR mice and the height of the ventral tuberculum (HVT) was significantly lower than that of ICR mice (Fig. 11). The shape of the ventral tuberculum was consistently flat and wide in comparison with that of ICR mice (Fig. 12). In the 6th cervical vertebra, the greatest thickness of the ventral lamina (GTVL) was nearly twice that of ICR mice (Fig. 13), and the shape seemed to be broader than that of ICR mouse (Fig. 14).

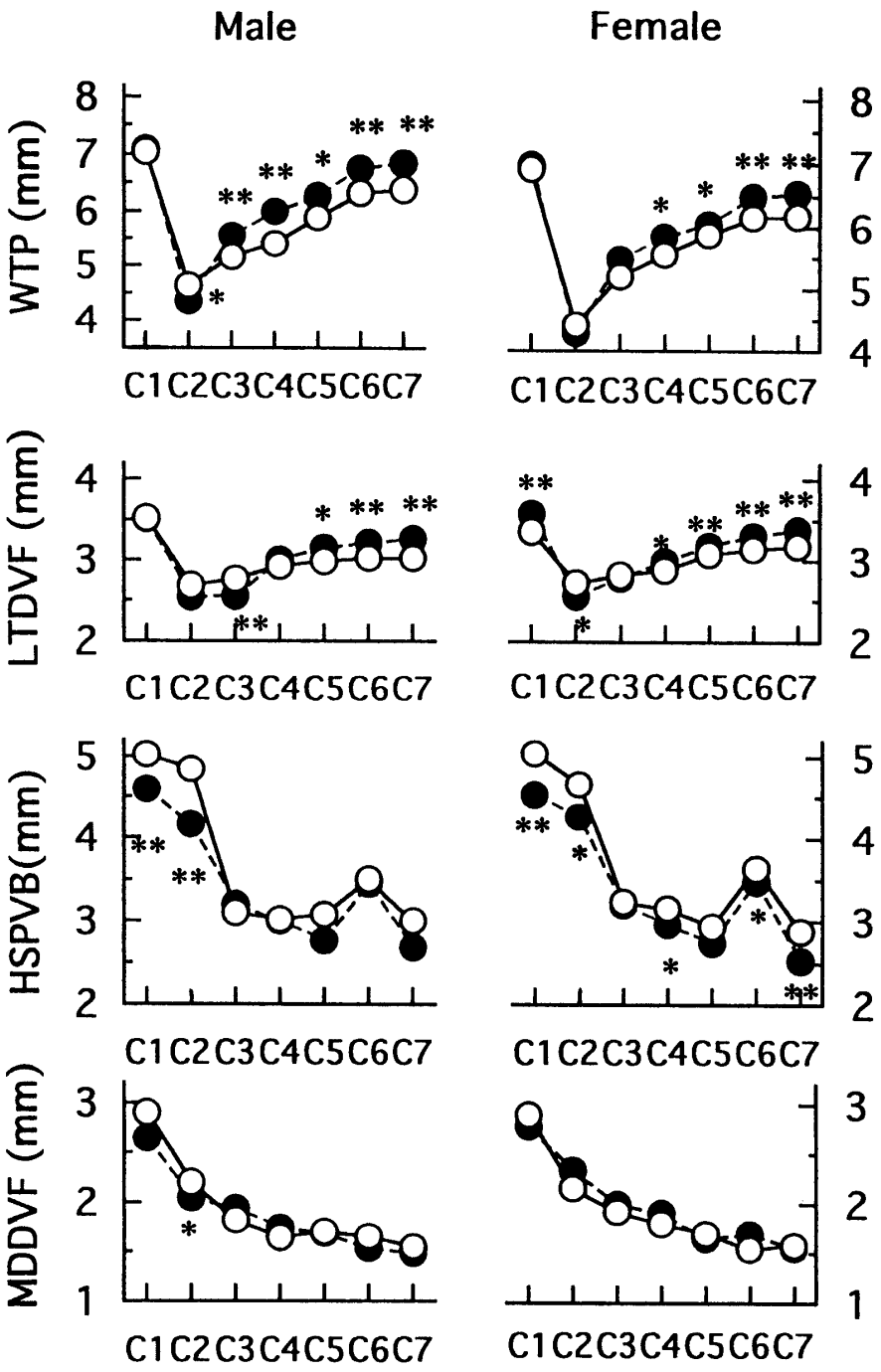

Fig. 9 Morphometric analyses on all the cervical vertebrae and their foramen of 52-week-old mice.
WTP, the width across the transverse processes; **LTDVF**, the longest transverse diameter of the vertebral foramen; **HSPVB**, the height from the spinous process to the vertebral body; **MDDVF**, the median dorsoventral diameter of the vertebral foramen. See Fig. 1. **C**, Cervical vertebra; ○: ICR mice; ●: *knt/knt* mice; *: $P < 0.05$; **: $P < 0.01$ (significant difference from ICR mice). The WTP and the LTDVF of *knt/knt* mice are significantly and continuously greater from the 3rd or 4th cervical vertebra to the 7th cervical vertebra than in ICR mice. The HSPVB is significantly lower in atlas and axis.

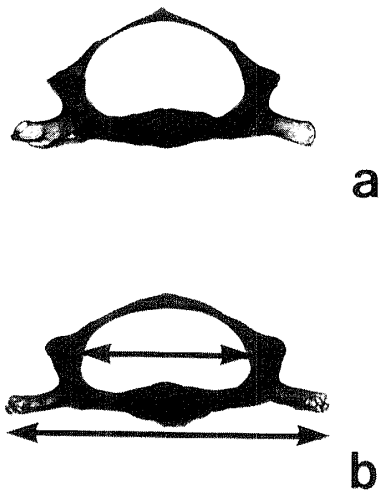

Fig. 10 Comparison of the cervical width indicated by soft X-ray examination in 52-week-old male mice. The specimen above (a) is a 7th cervical vertebra of a ICR mouse and the other (b) is that of a *knt/knt* mouse. The latter (*arrows*) seems to be wider than that of a ICR mouse. ×5.5.

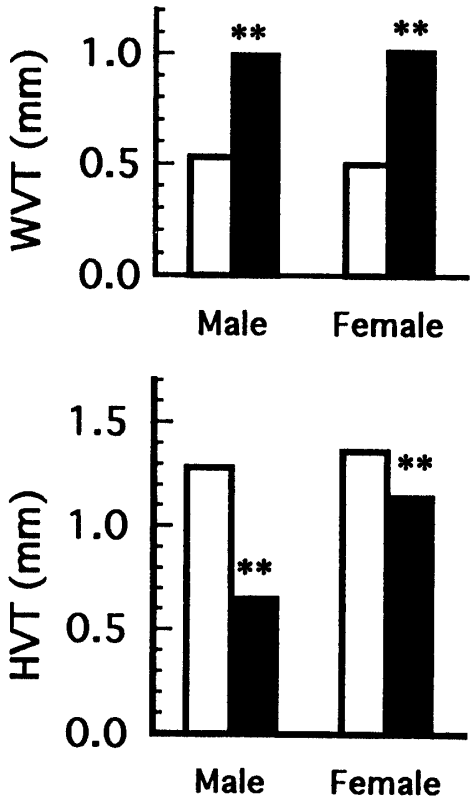

Fig. 11 Morphometric analyses on the atlas of 52-week-old mice.
WVT, the width of the ventral tuberculum; **HVT**, the height of the ventral tuberculum. See Fig. 2. □: ICR mice; ■: *knt/knt* mice; **: $P < 0.01$ (significant difference from ICR mice). The WVT of *knt/knt* mice is nearly twice that of ICR mice and the HVT is significantly lower than that of ICR mice.

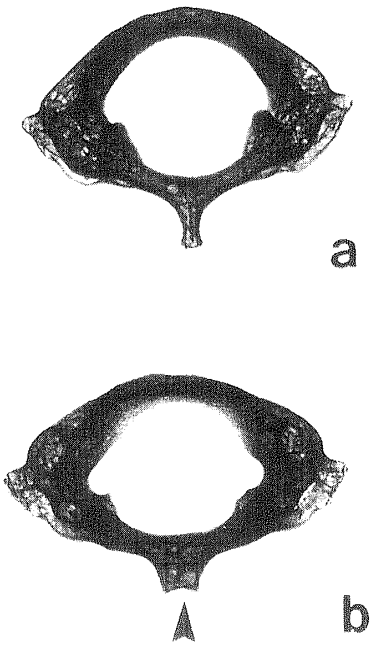

Fig. 12 Structure of the atlas indicated by soft X-ray examination in 52-week-old male mice. The specimen above (a) is an atlas of a ICR mouse and the other (b) is that of a *knt/knt* mouse. The ventral tuberculum of *knt/knt* mouse (*arrowhead*) is flat and wide in comparison with that of a ICR mouse. ×5.5.

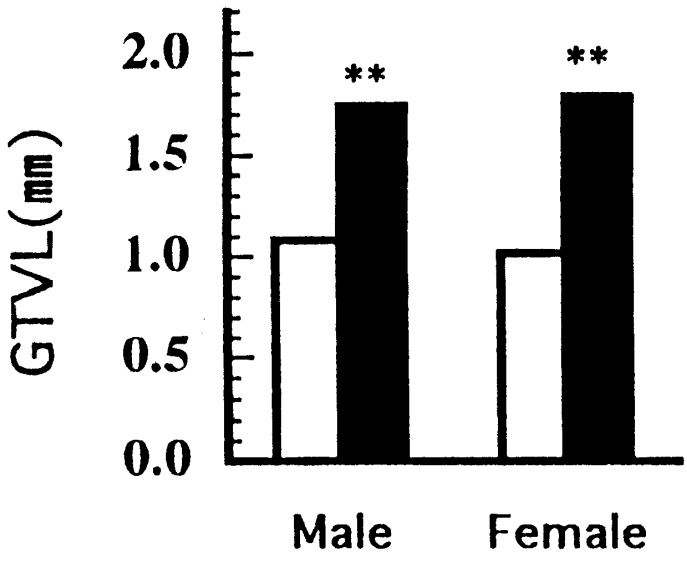

Fig. 13 Morphometric analyses on the 6th cervical vertebra of 52-week-old mice.
GTVL, the greatest thickness of the ventral lamina. See Fig. 2. □: ICR mice; ■: *knt/knt* mice; **: $P < 0.01$ (significant difference from ICR mice). The GTVL of *knt/knt* mice is nearly twice that of ICR mice.

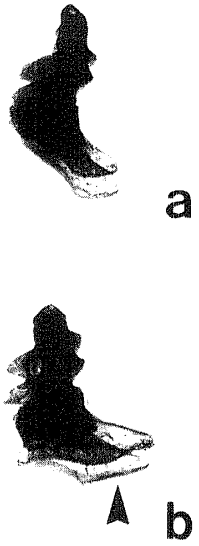

Fig. 14 Structure of the 6th cervical vertebra indicated by soft X-ray examination in 52-week-old male mice. The specimen above (a) is a 6th cervical vertebra of a ICR mouse and the other (b) is that of a *knt/knt* mouse. The ventral lamina of *knt/knt* mouse (*arrowhead*) seems to be broader than that of a ICR mouse. ×5.5.

DISCUSSION

From the observation of double-stained preparations of *knt/knt* mice in this study, morphological changes of cervical vertebrae were confined to the vertebral arch of the axis, which was usually asymmetrical and hypoplastic. The cervical deformities involving the axis have been reported in other mutants, including *Mv/+* (Theiler et al., 1975), *pu/pu* (Grüneberg, 1961), *rh/rh* (Theiler et al., 1974) , *Tc/+* (Searle, 1966) and *tk/tk* (Grüneberg, 1955). However, these are extremely severe anomalies such as fusions involving any or all cervical vertebrae, or chaotic fragmentation, which makes it impossible to distinguish individual vertebra (Theiler, 1988). The deformities of the axis in *knt/knt* mice are much less severe than those of the other mutant mice, and the gene responsible for the axis anomaly is considered to be different from other genes.

From the morphometric analyses, minor anomalies (i.e., broadened cervical vertebrae in the transverse direction, shortened and broadened ventral tuberculum of the atlas, thickened ventral lamina of 6th cervical vertebra) were detected in the cervical vertebrae of 52-week-old *knt/knt* mice outside of the axis. These characteristics, which have been also confirmed in 5-week-old *knt/knt* mice (Matsuura et al., 1997), are considered to be maintained with advancing age as well, and are peculiar to this strain.

It is also evident from the study that a morphological deformity, reflecting an adult osseous anomaly in *knt/knt* mice, had been already formed in the cartilaginous axis prenatally. These findings agree with changes in the axis of fetuses of other mutant mice. In *Ts /+* mice, many of the abnormalities of the osseous skeleton of the adult can be seen in the cartilaginous skeleton of 14- to 17-day embryos (Deol, 1961). Moreover, in *tk/tk* mice the osseous skeleton simply repeats the deformities already present in the cartilaginous skeleton (Grüneberg, 1955). Therefore, it is highly probable that an anomaly of the axis in *knt/knt* mice would be caused by a disturbance in coalescence (abnormal chondrogenesis) of the paired laminae at the midline, as a result of which the formation of the spinous process may be also disturbed.

In both humans and animals, cervical vertebral anomalies are mainly classified into three groups: (1) occipitalization of the atlas, (2) abnormal odontoid process of the axis, and (3) stenosis of the cervical vertebral canal. Occipitalization of the atlas in human (Gunther, 1980; Smoker, 1994) and occipitoatlantoaxial malformations in Arabian horses (Mayhew et al., 1978) and Saint Bernard dogs (Watson et al., 1988) are the most commonly recognized anomaly of the craniovertebral junction. An abnormal odontoid process is often confirmed in human (Davis and Gutierrez, 1977; Smoker, 1994), in old or a breed of small dogs (Denny et al., 1977), and in *Tc/+* and *Sd/+* mice (Searle, 1966; Theiler, 1951). Stenosis of the cervical vertebral canal is well reported in young horses (Mayhew et al., 1993; Tomizawa et al., 1994), and in a breed of large dogs (Masson, 1979; Lincoln, 1992). Comparing with these previously reported cervical anomalies, the craniovertebral junction was normal in *knt/knt* mice, the odontoid process was almost morphologically and quantitatively the same as in normal ICR mice, and the cervical canal had a rather larger transverse diameter than ICR mice and showed no stenosis. The axis anomaly confirmed in this study does not belong to any of the above major types of cervical vertebral anomalies after all.

In the papain-digested preparations of *knt/knt* mice, a typical bony invagination into the canal was detected in the axis, and the morphometric analyses on axis revealed that the growth of spinous process was disturbed in comparison with that of ICR mice. Recently, computed tomography (CT) makes it possible to detect a three-dimensional profile of the dysplastic axis in the human cases. In one case, CT revealed the anomalous axis with spina bifida occulta and a pair of osseous fragments which are separated from the lamina of the arch of the axis on each side, and invaginate into the spinal canal causing myelopathy (Koyama et al., 1986). In another case, rare agenesis of the vertebral arch of the axis was confirmed (Bernini and Muras, 1985). In human cases, an invagination of osseous fragments into the axis canal was detected not by plain radiograph but only by a three-dimensional computed tomographic study (Koyama et al., 1986). It would seem, therefore, that these human axis anomalies greatly resemble those of *knt/knt* mice mentioned above and that humans may have more potential anomalies in the vertebral arch of the axis. While developmental analyses of the abnormal arch of human axis have never been done, the human axis anomalies detected by CT are expected to be similar in morphogenesis to *knt/knt* mice. In that case, *knotty-tail* mice are considered to be a suitable model for an anomalous axis in humans.

REFERENCES

Bernini, F.P. and Muras, I. (1985) Case report 332: A complex anomaly of the craniovertebral junction representing a regressive malformation with agenesis of the neural arch of C-2, hypomorphogenesis at C5-C6 and instability of the upper cervical spine. Skeletal Radiol., **14:** 226–230.

Crary, D.D. and Fox, R.R. (1983) Narrow axis: an inherited anomaly of the second cervical vertebra in the rabbit. J. Hered., **74:** 47–50.

Davis, D. and Gutierrez, F.A. (1977) Congenital anomaly of the odontoid in children. A report of four cases. Child's Brain, **3:** 219–229.

Denny, H.R., Gibbs, C. and Gaskell, C.J. (1977) Cervical spondylopathy in the dog - a review of thirty-five cases. J. Small Anim. Pract., **18:** 117–132.

Deol, M.S. (1961) Genetical studies on the skeleton of the mouse XXVIII. Tail short. Proc. R. Soc. Lond. (Biol)., **155**: 78–95.

Grüneberg, H. (1955) Genetical studies on the skeleton of the mouse. XVI. Tail-kinks. J. Genet., **53:** 536–550.

Grüneberg, H. (1961) Genetical studies on the skeleton of the mouse. XXIX. Pudgy. Genet. Res., **2:** 384-393.

Gunther, S.F. (1980) Congenital anomaly of the cervical spine: fusion of the occiput, atlas, and odontoid process. A case report. J. Bone Joint Surg. Am., **62:** 1377–1378.

Inouye, M. (1976) Differential staining of cartilage and bone in fetal mouse skeleton by Alcian Blue and

Alizarin Red S. Cong. Anom., **16:** 171–173.

Koyama, T., Tanaka, K. and Handa, J. (1986) A rare anomaly of the axis: report of a case with shaded three-dimensional computed tomographic display. Surg. Neurol., **25:** 491–494.

Lincoln, J.D. (1992) Cervical vertebral malformation/malarticulation syndrome in large dogs. Vet. Clin. North Am. Small Anim. Pract., **22:** 923–935.

Luther, P.G. (1949) Enzymatic maceration of skeletons. Proceedings of the Linnaean Society, **161:** 146–147.

Masson, T.A. (1979) Cervical vertebral instability (wobbler syndrome) in the dog. Vet. Rec., **104:** 142–145.

Matsuura, T., Narama, I., Nishikawa, T., Nishimura, M., Imagawa, T., Kitagawa, H. and Uehara, M. (1997) Morphological and morphometric features of the deformed cervical and caudal vertebrae in a new mutant *knotty-tail* (*knt/knt*) mouse. Ann. Anat., **179:** 277–283.

Mayhew, I.G., Donawick, W.J., Green, S.L., Galligan, D.T., Stanley, E.K. and Osborne, J. (1993) Diagnosis and prediction of cervical vertebral malformation in thoroughbred foals based on semi-quantitative radiographic indicators. Equine Vet. J., **25:** 435–440.

Mayhew, I.G., Watson, A.G. and Heissan, J.A. (1978) Congenital occipitoatlantoaxial malformations in the horse. Equine Vet. J., **10:** 103–113.

Searle, A.G. (1966) Curtailed, a new dominant T-allele in the house mouse. Genet. Res., **7:** 86–95.

Smoker, W.R. (1994) Craniovertebral junction: normal anatomy, craniometry, and congenital anomalies. Radiographics, **14:** 255–277.

Theiler, K. (1951) Die Entstehung der Densluxation bei der Short Danforth-Maus. Arch. Julius Klaus-Shiftung Verteb Forschung, **26:** 450–454.

Theiler, K. (1988). Vertebral malformations. Springer-Verlag, Berlin, Heidelberg.

Theiler, K., Varnum, D., Southard, J.L. and Stevens, L.C. (1975) Malformed vertebrae: a new mutant with the "Wirbel-Rippen Syndrom" in the mouse. Anat. Embryol., **147:** 161–166.

Theiler, K., Varnum, D.S. and Stevens, L.C. (1974) Development of rachiterata, a mutation in the house mouse with 6 cervical vertebrae. Z. Anat. Entwickl.-Gesch., **145:** 75–80.

Tomizawa, N., Nishimura, R., Sasaki, N., Nakayama, H., Kadosawa, T., Senba, H. and Takeuchi, A. (1994) Relationships between radiography of cervical vertebrae and histopathology of the cervical cord in wobbling 19 foals. J. Vet. Med. Sci., **56:** 227–233.

Watson, A.G., Lahunta, A. and Evans, H.E. (1988) Morphology and embryological interpretation of a congenital occipito-atlanto-axial malformation in a dog. Teratology, **38:** 451–459.